# Vibronic-coupling effect on the paramagnetic $Fe^{2+}$ ions in an insulator: Mössbauer quadrupole splitting in a biological system

T. P. Sinha

*Solid State and Molecular Physics Division, Saha Institute of Nuclear Physics, 1/AF, Bidhan Nagar Calcutta 700064, India*

(Received 4 September 1991; revised manuscript received 28 January 1992)

The temperature variation of the Mössbauer quadrupole splitting of $Fe^{2+}$ ions in deoxygenated myoglobin, deoxygenated hemoglobin, and its structurally similar synthetic analogues have been theoretically analyzed, with the effect of orbit-lattice interaction taken into account. The present study considers $Fe^{2+}$ in the high-spin ($S=2$) configuration only and then uses the vibronic coupling as a perturbation that effectively produces mixings between the otherwise static crystal-field orbital states. This results in a better agreement between theoretical and experimental data. It shows that the effect of orbit-lattice interaction should be duly included in the interpretation of Mössbauer observables as a function of the temperature in biological complexes.

## I. INTRODUCTION

The Mössbauer parameters, magnetic susceptibility, and x-ray data have been widely used to study the low-energy electronic states of Fe(II) in biological complexes like deoxygenated myoglobin, deoxygenated hemoglobin, and its structurally similar synthetic analogues.[1-20] The main results of these studies are: (i) The magnitude of quadrupole splitting at 4.2 K ($QS \sim 2.3$ mm/sec) and the isomer shift ($IS \sim 1.0$ mm/sec) indicates a high-spin ($S=2$) configuration for the $Fe^{2+}$ ions, (ii) $QS$ decreases considerably with temperature, (iii) the largest principal potential second derivative $V_{zz}$ (the principal component of the electric-field gradient) is $-ve$, and the asymmetry parameter $\eta$ is temperature independent, (iv) the hyperfine field ($HF \sim 11$ T) is much smaller than expected from $S=2$ with no ground orbital moment, (v) the ferrous ion has a nearly square pyramidal structure corresponding to $C_{4v}$ site symmetry, and (vi) the low-temperature magnetic susceptibility corresponds to $S=2$.[21] A theoretical scheme which can explain all these observed results consistently is still lacking.

Several investigators have suggested electronic level schemes for fitting some or all of the above data. Eicher and Trautwein[1] included all possible electronic states arising from $S=2,1,0$ to explain the temperature dependence of the quadrupole splitting and magnetic susceptibility in a reasonable manner. The calculations of Huynh *et al.*[5] and Eicher, Bade, and Parak[13] were based on the crystal-field approximation, while Trautwein, Zimmermann, and Harris[10] used molecular orbital techniques. Bacci[15] proposed a theoretical scheme which considered only the high-spin $Fe^{2+}$ situated under a crystal-field potential of $C_{4v}$ site symmetry along with a weak Jahn-Teller and vibronic interaction of a discrete frequency. All these proposed models have one common feature, that is, the largest component of the electric-field gradient was taken to be $+ve$. However, the experimental results of Kent and co-workers[18-20] under an applied magnetic field of 6 T give contrary evidence. This makes the approach of earlier workers suspect. Huynh and Kent[21] have discussed these points quite elaborately and indicated the inadequacy of the existing theoretical scheme in explaining simultaneously the temperature dependence of the quadrupole splitting, the magnetic susceptibility, and a low value of the hyperfine field at the Fe nucleus in deoxyhemoglobin and myoglobin. It is therefore obvious that a reinterpretation of the observed data is needed.

In the present theoretical work, an attempt has been made to explain the temperature dependence of the quadrupole splitting by taking into account the effect of orbit-lattice interaction (or vibronic coupling) as a perturbation over the appropriate static crystal-field potential, which is expected to be as important in these biological systems with low Debye temperatures as in the case of inorganic and organometallic systems.[22-27] This approach has the definite advantage of considering the $Fe^{2+}$ ($3d^6, {}^5D$) ions with the high-spin configuration only, which avoids the multitude of electronic energy levels when different spin configurations are included. In the following sections first of all we have derived the correct form of crystal-field potential from the coordinates of the ligands around $Fe^{2+}$ ions in the deoxyhemoglobin structure and used the same to obtain the crystal-field orbital states. The temperature variation of quadrupole splitting has been roughly calculated from these levels and then dynamic crystal-field potential has been used as a perturbation to improve the agreement between theoretical and experimental data in a very natural manner.

## II. STRUCTURE OF HEMOGLOBIN

Hemoglobin occurs in all vertebrates (with some exceptions) and in many invertebrates; it has also been found in certain strains of yeasts, molds, etc. It is a chromoprotein, the protein part being globin (94%) and the prosthetic group being Heme (6%). The composition of hemoglobin varies slightly, depending on the species from

which it is isolated; the variation occurs only in the globin part of the molecule.

The way in which the globin part is bound to heme has been the subject of much discussion. Globin consists of four polypeptide chains, and in human hemoglobin the chains are of two types which have different terminal acid groups: $\alpha$ chain, valyl-leucyl end group; $\beta$ chain, valyl-histidyl-leucyl end group. Normal adult hemoglobin contains two $\alpha$ chains (141 amino acids each) and two $\beta$ chains (146 amino acids each).

Heme is an iron protoporphyrin complex. When the iron atom is in the ferrous state, the complex is called "ferrous protoporphyrin," or "heme," and the molecule is electrically neutral. When the iron atom is in the ferric state, the complex is called "ferric protoporphyrin," or "hemin," and the molecule carries a unit positive charge (and is consequently associated with an anion). In the animal body, hemoglobin readily combines with oxygen to form "oxyhemoglobin."

In heme the four ligands (the four pyrrole groups) form a square planar complex (via the nitrogen atoms). The two remaining positions of coordination are perpendicular to this plane (i.e., the plane of the prophyrin ring) as shown in Fig. 1. Hemoglobin contains four molecules of heme for each molecule of globin (which consists of two $\alpha$ and two $\beta$ chains). Each iron atom (ferrous) has formed a square planar complex with the protoporphyrin molecule, and a fifth position is occupied by an imidazole ring (of the histidine amino acid residue). It appears that the ring atom is bound to histidine-87 in the $\alpha$ chain and to histidine-92 in the $\beta$ chain. Furthermore, it has been shown that each heme molecule is embedded in one of the four chains of the globin molecule.

If the sixth ligand of the ferrous ion is unoccupied, the arrangement is a square pyramid. This is considered to be the case with hemoglobin, but it is possible that the sixth position is occupied by a water molecule, resulting in an octahedral complex. In either case, when hemoglobin combines with one molecule of oxygen to form oxyhemoglobin, it is this sixth position which coordinates with the oxygen molecule (the iron atom is still in the ferrous state); the water molecule, if present in hemoglobin, is readily displaced. The various hemoglobin compounds are all derivatives of the parent substance known as "porphin." Substituted porphins are known as porphyrins.

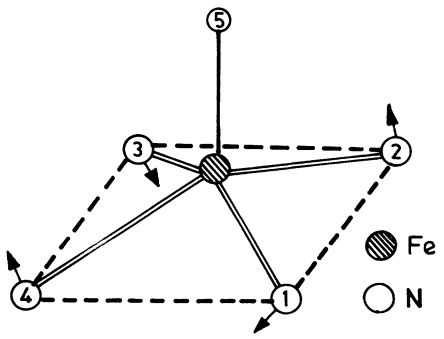


FIG. 1. Iron coordination symmetry in deoxyhemoglobin and myoglobin.

Hemoglobin and myoglobin are very similar compounds having almost identical structure and therefore all the discussion pertaining to hemoglobin remains applicable more or less to myoglobin.

## III. ELECTRONIC STATES OF Fe (II)

The x-ray studies of deoxyhemoglobin show that the ferrous ion has a nearly square pyramidal structure corresponding to $C_{4v}$ site symmetry[3,8] and is coordinated to five nitrogen ligands as shown in Fig. 2. Assuming $C_{4v}$ point symmetry of the ferrous ion, the coordinates of iron(II), *N*-imidazol, and the four pyrrole nitrogens in the heme plane are expressed in Cartesian and spherical polar coordinates as

$$\text{Fe: } (0,0,0) ,$$

$$\text{N(1): } (a,0,-b);\ (\sqrt{a^2+b^2},\theta,0) ,$$

$$\text{N(2): } (-a,0,-b);\ (\sqrt{a^2+b^2},\theta,\pi/2) ,$$

$$\text{N(3): } (0,a,-b);\ (\sqrt{a^2+b^2},\theta,\pi) ,$$

$$\text{N(4): } (0,-a,-b);\ (\sqrt{a^2+b^2},\theta,3\pi/2) ,$$

$$\text{N(5): } (0,0,c);\ (c,0,0) ,$$

where

$$\theta=\pi/2+\alpha \quad \text{and} \quad \sin\alpha=\frac{b}{\sqrt{a^2+b^2}} . \tag{1}$$

The Fe ion is above the $x$-$y$ plane, i.e., it is displaced at a distance $b$ toward the $z$ direction above the $x$-$y$ plane, as shown in Fig. 2.

The crystal-field potential at the $Fe^{2+}$ ion is given by[28–31]

$$V(r)=B_4^0O_4^0+B_4^4O_4^4+B_2^0O_2^0+B_2^2O_2^2 , \tag{2}$$

where $B_n^m$ ($n=2,4$ and $m=0,2,4$) are the static crystal-field parameters and the operators $O_n^m$ are compiled by

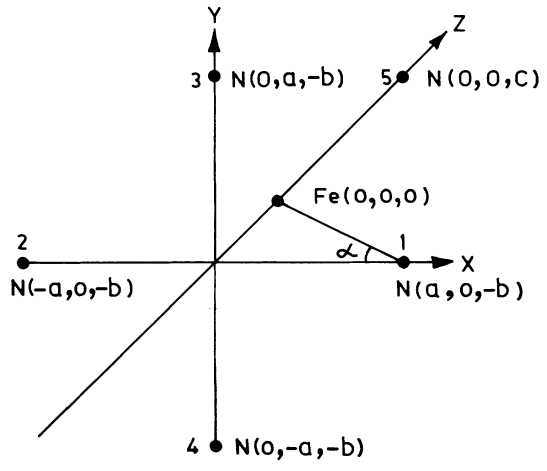


FIG. 2. Coordinates of iron(II), *N*-imidazol, and four pyrrole nitrogens in the heme plane.

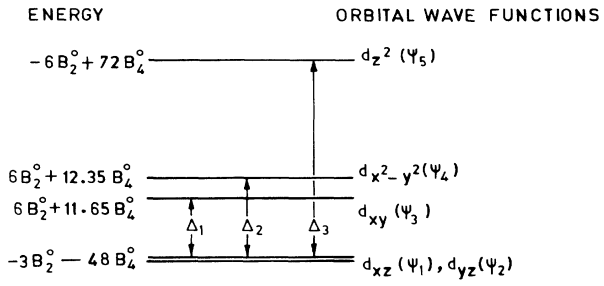


FIG. 3. Energy-level scheme of Fe(II) in deoxyhemoglobin.

Orbach[31] and Hutchings[30] in a standard form. The term $B_2^2O_2^2$ is needed if a rhombic distortion is considered. Using $a=2.02$ Å, $b=0.49$ Å, and $c=2.00$ Å for deoxyhemoglobin,[13] one gets the relation $34B_4^4=B_4^0$.

The $^5D$ state of a free $Fe^{2+}$ ion is split up by this crystal-field interaction, as given in Fig. 3. The electronic orbital states are represented as

$$\begin{aligned} d_{xz}(\psi_1)&=-(1/\sqrt{2})[|1\rangle-|-1\rangle]\ , \\ d_{yz}(\psi_2)&=(i/\sqrt{2})[|1\rangle+|-1\rangle]\ , \\ d_{xy}(\psi_3)&=-(i/\sqrt{2})[|2\rangle-|-2\rangle]\ , \\ d_{x^2-y^2}(\psi_4)&=(1/\sqrt{2})[|2\rangle+|-2\rangle]\ , \\ d_{z^2}(\psi_5)&=|0\rangle\ , \end{aligned} \tag{3}$$

and the energy separations are given by

$$\begin{aligned} \Delta_1&=9B_2^0+59.65B_4^0\ , \\ \Delta_2&=9B_2^0+60.35B_4^0\ , \\ \Delta_3&=-3B_2^0+120B_4^0\ . \end{aligned} \tag{4}$$

The optical absorption spectra of this compound show an absorption band at around 15 835 $cm^{-1}$,[32] which corresponds to $\Delta_3$. For this value of $\Delta_3$, $B_2^0$ and $B_4^0$ can be evaluated for a given value of $\Delta_1$ (which is not obtained from optical spectra because of its small values). Hence we will keep $\Delta_1$ as a variable parameter.

This crystal-field scheme will fulfill the condition that the quadrupole interaction must have $-ve$ sign, which is the case with the ground doublet $(d_{xz},d_{yz})$. The only other orbital state which has got $-ve$ quadrupole interaction is $d_{z^2}$ and on this basis it has also been suggested that the ground-state wave functions should be like $d_{z^2}$.[21] However, this does not follow from the crystal-field approach. In fact the state $d_{z^2}$ could possibly become ground state only when the site symmetry of $Fe^{2+}$ is either tetrahedral or trigonal. Therefore, it is more realistic to assume that the ground state consists of a doublet $(d_{xz},d_{yz})$ for the site symmetry $C_{4v}$. This is also supported by the magnitude of the observed quadrupole splitting ($\Delta E_Q\sim 2.40$ mm/sec) in these compounds. It can be easily seen that the quadrupole splitting produced by $d_{z^2}$ is twice that produced by the doublet $(d_{xz},d_{yz})$ at very low temperatures ($T\rightarrow 0$ K). The magnitude of the observed quadrupole splitting is $\sim 3.5$ mm/sec at low temperatures when $d_{z^2}$ is the ground state as in the case of ferrous fluosilicate.[33]

## IV. STATIC CRYSTAL-FIELD SCHEME

An attempt was made to fit the observed data with this energy-level scheme keeping $\Delta_1\simeq\Delta_2$ as a variable. The level at $\Delta_3$ was not considered because of its very high energy (i.e., its contribution will be negligible at temperatures of interest). For these four levels, the thermal average of the electric-field gradient (EFG) and asymmetry parameter will be[34]

$$\begin{aligned} \langle V_{zz}\rangle_T&=\frac{-2}{7}|e|\langle r^{-3}\rangle \\ &\times\frac{2-2\exp(-\Delta_1/k_BT)-2\exp(-\Delta_2/k_BT)}{2+\exp(-\Delta_1/k_BT)+\exp(-\Delta_2/k_BT)} \end{aligned}$$

and (5)

$$\langle \eta V_{zz}\rangle_T=0\ .$$

The quadrupole splitting at any temperature will be given by[34]

$$(\Delta E_Q)_T=\frac{eQ}{4I(2I-1)}\left[\langle V_{zz}\rangle_T^2+\frac{1}{3}\langle \eta V_{zz}\rangle_T^2\right]^{1/2}\ ,$$

where $Q$ is the nuclear quadrupole moment of $^{57}Fe$, and $I$ the nuclear-spin operator.

Finally, it can be written as

$$\begin{aligned} (\Delta E_Q)_T&=(\Delta E_Q)_0 \\ &\times\frac{2-2\exp(-\Delta_1/k_BT)-2\exp(-\Delta_2/k_BT)}{2+\exp(-\Delta_1/k_BT)+\exp(-\Delta_2/k_BT)}\ , \end{aligned} \tag{6}$$

where

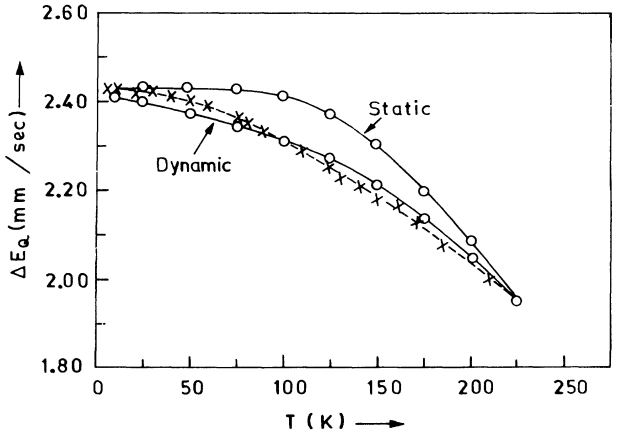


FIG. 4. Temperature variation of the quadrupole splitting of Fe(II) in deoxyhemoglobin: ×, Experimental points; ○, theoretical points.

$$(\Delta E_Q)_0 = \frac{-2}{7}|e|\langle r^{-3}\rangle \frac{eQ}{4I(2I-1)}$$

$$= \text{quadrupole splitting at 0 K} .$$

The best possible agreement of the temperature variation of the quadrupole splitting for $\Delta_1 \sim 420$ cm$^{-1}$ is shown in Fig. 4. It is obvious that the agreement is not very reasonable, and one needs much improvement.

## V. SITUATION FOR NONDEGENERATE $d_{xz}$ AND $d_{yz}$

If one assumes that the doublet $(d_{xz}, d_{yz})$ splits because of some rhombic distortion, Jahn-Teller effect, or any other interaction, the term $B_2^2 O_2^2$ of the crystal-field potential will be considered and the situation will correspond to a four-level problem having $d_{xz} < d_{yz} < d_{xy} < d_{x^2-y^2}$. In this case, the quadrupole splitting at any temperature will be given by[34]

$$(\Delta E_Q)_T = \frac{(\Delta E_Q)_0}{2[1+\exp(-\varepsilon_1/k_BT)+\exp(-\varepsilon_2/k_BT)+\exp(-\varepsilon_3/k_BT)]} \times \{[1+\exp(-\varepsilon_1/k_BT)-2\exp(-\varepsilon_2/k_BT)-2\exp(-\varepsilon_3/k_BT)]^2+\tfrac{1}{3}[3-3\exp(-\varepsilon_1/k_BT)]^2\}^{1/2} , \quad (7)$$

where $\varepsilon_1$, $\varepsilon_2$, and $\varepsilon_3$ are the energy gaps between levels $d_{xz}$ and $d_{yz}$, $d_{xz}$ and $d_{xy}$, and $d_{xz}$ and $d_{x^2-y^2}$, respectively.

The temperature variation of the quadrupole splitting given by this expression (7) is much more drastic than given by the expression (6) for the degenerate ground state. For example, if one chooses $\varepsilon_1 \simeq 100$ cm$^{-1}$ and $\varepsilon_2 \simeq \varepsilon_3 \simeq 400$ cm$^{-1}$, it can be easily seen that the quadrupole splitting decreases by a factor of almost $\frac{1}{2}$ as the temperature increases from 4.2 to 200 K. This is quite contrary to the observed data. It can be easily seen that if, at all, one assumes a splitting between $d_{xz}$ and $d_{yz}$, this splitting should be either of the order of 300–400 cm$^{-1}$ (which is very high) or less than 10 cm$^{-1}$ (which is very, very small). An intermediate value of this splitting is not consistent with the experimental results. The presence of any strong rhombic distortion is not realistic in view of the site symmetry ($C_{4v}$) of $Fe^{2+}$ in the molecule concerned; it is natural that the levels $d_{xz}$ and $d_{yz}$ will be regarded as degenerate, which will be consistent with the x-ray structure and the observed temperature variation of the quadrupole splitting.

## VI. CONSIDERATION OF SPIN-ORBIT COUPLING

The spin-orbit coupling $\lambda L \cdot S$ removes the orbital degeneracy of the ground doublet $(d_{xz}, d_{yz})$ and also produces a substantial mixing with states $d_{xy}$ and $d_{x^2-y^2}$. The 20-basis spin-orbital states are the product functions $|M_L, M_S\rangle$ (where $M_L = d_{xz}, d_{yz}, d_{xy}, d_{x^2-y^2}$, and $M_S = \pm 2, \pm 1, 0$) and in general the electronic eigenfunctions will be linear combinations of these basis states. To include vibronic coupling between all these electronic states is a potentially complicated problem, but, as pointed out by Price[35] and Sinha and co-workers,[25,26] the essential features of the problem can be retained by assuming the spin degeneracy to be equal to 2, say $M_S = \pm 2$ only. This will eliminate the off-diagonal terms arising from $(\lambda/2)(L_+S_- + L_-S_+)$, but at the same time remove the orbital degeneracy. In effect one obtains four doublets given by $|d_{xz}, \pm 2\rangle$, $|d_{yz}, \pm 2\rangle$, $|d_{xy}, \pm 2\rangle$, and $|d_{x^2-y^2}, \pm 2\rangle$ in order of increasing energy. The components of EFG obtained from these states are used to calculate the net quadrupole splitting. Because both the components of a given doublet produce identical EFG, the thermal average of the EFG will remain the same as can be obtained by considering only four states with $M_S = 2$ or $-2$. This gives the same situation as discussed in Sec. V and hence there is no possibility of any further splitting of the energy levels due to spin-orbit coupling.

Once the energy-level scheme for the dominant crystal-field interaction has been finalized (Fig. 3), the effect of orbit-lattice interaction will now be considered as a small perturbation.

## VII. INFLUENCE OF ORBIT-LATTICE INTERACTION

In the long photon wavelength approximation the orbit-lattice interaction is represented as[31,36]

$$H_{ol} = \sum_k \sum_{n,m} \left[\frac{\hbar}{2M\omega_k}\right]^{1/2} k V_n^m(L)(a_k + a_k^*) , \quad (8)$$

where the terms have their usual meaning[22] and the phonon spectrum is isotropic.

The vibronically perturbed electronic states can be obtained by the first order perturbation method and given by

$$\psi_1 = A_1 \left[ |d_{xz}, n_k\rangle + \frac{\langle d_{xz}, n_k | H_{ol} | d_{xy}, n_k+1\rangle}{\Delta_1 + \hbar\omega_k} |d_{xy}, n_k+1\rangle + \frac{\langle d_{xz}, n_k | H_{ol} | d_{xy}, n_k-1\rangle}{\Delta_1 - \hbar\omega_k} |d_{xy}, n_k-1\rangle \right.$$
$$\left. + \frac{\langle d_{xz}, n_k | H_{ol} | d_{x^2-y^2}, n_k+1\rangle}{\Delta_2 + \hbar\omega_k} |d_{x^2-y^2}, n_k+1\rangle + \frac{\langle d_{xz} n_k | H_{ol} | d_{x^2-y^2}, n_k-1\rangle}{\Delta_2 - \hbar\omega_k} |d_{x^2-y^2}, n_k-1\rangle \right] , \quad (9)$$

where $A_1$ is the normalization constant and $n_k$ the phonon occupation number.

Now it is seen that

$$\langle d_{xz}, n_k | H_{ol} | d_{xy}, n_k \pm 1 \rangle = 0 , \tag{10}$$

because the sum of the matrix elements over the crystal-field term ($\sum V_n^m$) becomes zero.

Further, it can be shown that

$$\begin{aligned} \left\langle d_{xz} \left| \sum_{n,m} V_n^m \right| d_{x^2-y^2} \right\rangle &= -1.5C_2^1 - 3C_4^1 + 3C_4^3 , \\ \left\langle d_{yz} \left| \sum_{n,m} V_n^m \right| d_{xy} \right\rangle &= 1.5C_2^1 + 3C_4^1 + 3C_4^3 , \\ \left\langle d_{yz} \left| \sum_{n,m} V_n^m \right| d_{x^2-y^2} \right\rangle &= 0 , \end{aligned} \tag{11}$$

and

$$\left\langle d_{xy} \left| \sum_{n,m} V_n^m \right| d_{x^2-y^2} \right\rangle = 0 ,$$

where $C_n^m$ are the dynamic crystal-field parameters.

The dynamic and static crystal-field parameters, according to Huang's approximation[37] are related as

$$C_n^m \simeq (n+1) B_n^m ,$$

giving

$$C_2^1 \simeq 3B_2^0 \quad \text{and} \quad C_4^1 \simeq C_4^3 \simeq 5B_4^0 . \tag{12}$$

Thus,

$$\begin{aligned} \psi_1 = A_1 [ | d_{xz}, n_k \rangle + \alpha_1 | d_{x^2-y^2}, n_k + 1 \rangle \\ + \beta_1 | d_{x^2-y^2}, n_k - 1 \rangle ] , \end{aligned} \tag{13}$$

where

$$\alpha_1 = \frac{\langle d_{xz}, n_k | H_{ol} | d_{x^2-y^2}, n_k + 1 \rangle}{\Delta_2 + \hbar\omega_k}$$

and

$$\beta_1 = \frac{\langle d_{xz}, n_k | H_{ol} | d_{x^2-y^2}, n_k - 1 \rangle}{\Delta_2 - \hbar\omega_k} . \tag{14}$$

Similarly, the other vibronically perturbed electronic states can be represented as

$$\begin{aligned} \psi_2 &= A_2 [ | d_{yz}, n_k \rangle + \alpha_2 | d_{xy}, n_k + 1 \rangle + \beta_2 | d_{xy}, n_k - 1 \rangle ] , \\ \psi_3 &= A_3 [ | d_{xy}, n_k \rangle + \alpha_3 | d_{yz}, n_k + 1 \rangle + \beta_3 | d_{yz}, n_k - 1 \rangle ] , \end{aligned} \tag{15}$$

and

$$\psi_4 = A_4 [ | d_{x^2-y^2}, n_k \rangle + \alpha_4 | d_{xz}, n_k + 1 \rangle + \beta_4 | d_{xz}, n_k - 1 \rangle ] .$$

It is seen that

$$\alpha_1^2 + \beta_1^2 = \alpha_4^2 + \beta_4^2 \quad \text{and} \quad \alpha_2^2 + \beta_2^2 = \alpha_3^2 + \beta_3^2 . \tag{16}$$

The normalization constants are related as

$$\begin{aligned} A_1^2 = A_4^2 = [1 + (\alpha_1^2 + \beta_1^2)]^{-1} \\ \text{and} \\ A_2^2 = A_3^2 = [1 + (\alpha_2^2 + \beta_2^2)]^{-1} , \end{aligned} \tag{17}$$

where

$$\begin{aligned} \alpha_2 &= \frac{\langle d_{yz}, n_k | H_{ol} | d_{xy}, n_k + 1 \rangle}{\Delta_1 + \hbar\omega_k} , \\ \beta_2 &= \frac{\langle d_{yz}, n_k | H_{ol} | d_{xy}, n_k - 1 \rangle}{\Delta_1 - \hbar\omega_k} . \end{aligned} \tag{18}$$

In an earlier paper[22] the matrix elements over orbit-lattice interaction have been obtained by using the properties of the phonon annihilation and creation operators, and following the same procedure, one obtains that

$$\alpha_1^2 + \beta_1^2 = aI(T)T^4 \quad \text{and} \quad \alpha_2^2 + \beta_2^2 = bI(T)T^4 , \tag{19}$$

where

$$\begin{aligned} a &= \frac{\hbar}{4\pi^2 \rho v^5} \frac{\left| \left\langle d_{xz} \left| \sum_{n,m} V_n^m \right| d_{x^2-y^2} \right\rangle \right|^2}{\Delta_2^2} \left( \frac{k_B}{\hbar} \right)^4 , \\ b &= \frac{\hbar}{4\pi^2 \rho v^5} \frac{\left| \left\langle d_{yz} \left| \sum_{n,m} V_n^m \right| d_{xy} \right\rangle \right|^2}{\Delta_1^2} \left( \frac{k_B}{\hbar} \right)^4 , \end{aligned}$$

and

$$I(T) = \int_0^{\Theta_D/T} \frac{x^3 (e^x + 1)}{e^x - 1} dx . \tag{20}$$

$\rho$ is the density, $v$ the velocity of sound, and $\Theta_D$ the Debye temperature of the crystal. It has been assumed that $\Delta_1$ and $\Delta_2 \gg \hbar\omega_D$, where $\hbar\omega_D$ is the Debye energy.

Now the expectation values of the EFG operators are to be obtained for these vibronically perturbed states, keeping in mind that these operators connect only those electronic states for which the phonon occupation numbers are the same. Then one obtains that

$$\begin{aligned} \langle V_{zz} \rangle_{\psi_1} &= \langle \psi_1 | V_{zz} | \psi_1 \rangle \\ &= A_1^2 [ \langle d_{xz} | V_{zz} | d_{xz} \rangle + (\alpha_1^2 + \beta_1^2) \langle d_{x^2-y^2} | V_{zz} | d_{x^2-y^2} \rangle ] \\ &= A_1^2 [ -\tfrac{2}{7} |e| \langle r^{-3} \rangle + (\alpha_1^2 + \beta_1^2) \tfrac{4}{7} |e| \langle r^{-3} \rangle ] \\ &= -\frac{2}{7} |e| \langle r^{-3} \rangle \frac{1 - 2aI(T)T^4}{1 + aI(T)T^4} \end{aligned} \tag{21}$$

and

$$\langle \eta V_{zz} \rangle_{\psi_1} = \langle \psi_1 | V_{xx} - V_{yy} | \psi_1 \rangle = -\frac{2}{7} |e| \langle r^{-3} \rangle \frac{3}{1+aI(T)T^4} , \tag{22}$$

where we have used the standard values[34] of the EFG produced by pure orbitals.

In a similar fashion, one can obtain $\langle V_{zz} \rangle_{\psi_2}$, $\langle V_{zz} \rangle_{\psi_3}$, $\langle V_{zz} \rangle_{\psi_4}$, $\langle \eta V_{zz} \rangle_{\psi_2}$, $\langle \eta V_{zz} \rangle_{\psi_3}$, and $\langle \eta V_{zz} \rangle_{\psi_4}$. Finally, the Boltzmann thermal averages of $\langle V_{zz} \rangle$ and $\langle \eta V_{zz} \rangle$ are obtained. Using these, the quadrupole splitting at temperature $T$ is given by

$$\begin{aligned}(\Delta E_Q)_T = (\Delta E_Q)_0 & \frac{1}{2+\exp(-\Delta_1/k_BT)+\exp(-\Delta_2/k_BT)} \\ \times & \left[ \left[ \frac{1-2aI(T)T^4+[-2+aI(T)T^4]\exp(-\Delta_2/k_BT)}{1+aI(T)T^4} \right. \right. \\ & \left. + \frac{1-2bI(T)T^4+[-2+bI(T)T^4]\exp(-\Delta_1/k_BT)}{1+bI(T)T^4} \right]^2 \\ & \left. +3 \left[ \frac{1+aI(T)T^4\exp(-\Delta_2/k_BT)}{1+aI(T)T^4} - \frac{1+bI(T)T^4\exp(-\Delta_1/k_BT)}{1+bI(T)T^4} \right]^2 \right]^{1/2} .\end{aligned} \tag{23}$$

This is the final expression for the variation of quadrupole splitting with temperature.

## VIII. EVALUATION OF $(\Delta E_Q)_T$

The calculation of $(\Delta E_Q)_T$ requires a good estimation of various parameters.

It has been assumed that $(\Delta E_Q)_0 \simeq 2.43$ mm/sec, which is the measured value at 4.2 K, keeping in mind that the vibrational effect will be negligible at this temperature. In order to match the theoretical and experimental values of the quadrupole splitting, an approximate value of $\Delta = (\Delta_1 + \Delta_2)/2 \simeq 420$ cm$^{-1}$ has already been estimated from the static crystal-field scheme discussed in Sec. IV. We have generated several sets of theoretical values of $\Delta E_Q$ as a function of temperature by taking different values of $\Delta$ between 400 and 500 cm$^{-1}$. The static parameters $B_2^0$ and $B_4^0$ and hence $\Delta_1$ and $\Delta_2$ are each time derived for a given value of $\Delta$. The agreement appears fairly good for $\Delta = 500$ cm$^{-1}$ ($\Delta_1 \simeq 465$ cm$^{-1}$ and $\Delta_2 \simeq 535$ cm$^{-1}$). These values of $\Delta_1$ and $\Delta_2$ are quite reasonable and well within the expected range.

An experimental value of the Debye temperature in this compound is not available, however, it is expected to be very low. In the present calculations, the Debye temperature ($\Theta_D$) has been kept variable and each time the velocity of sound $v$ has been estimated from the standard phonon density-of-states relation

$$v^3 = \frac{VE_D^3}{6\pi^2\hbar^3 N} , \tag{24}$$

where $N$ is the number of molecules in volume $V$ and $E_D$ the Debye energy. The molecular weight of this compound is 616 g/mol, and the density $\rho \simeq 1.35$ g/cm$^3$, which corresponds to the molar volume $V = 456.3$ cm$^3$. The integral $I(T)$ was performed numerically for different values of Debye temperature between 30 and 75 K. It was found that for $\Theta_D \simeq 40$ K and correspondingly $v = 1.22 \times 10^5$ cm/sec, the agreement between calculated and observed values of $\Delta E_Q$ was quite fair. This value of Debye temperature is also well within the expected range. Using all these parameters, the $(\Delta E_Q)_T$ has been calculated as a function of temperature and compared with observed data as shown in Fig. 4.

It is worth mentioning that formula (23) involves a two-parameter fit ($\Delta$ and $\Theta_D$). A greater value of $\Delta$ requires a smaller value of $\Theta_D$ and vice versa. The theoretical data generated by using slightly different values of $\Delta$ and $\Theta_D$ (mentioned above) produce very similar types of temperature dependence of $\Delta E_Q$, but with somewhat different degrees of matching with the experimental data.

## IX. CONCLUSIONS

The overall agreement between the theoretical and experimental data between 4.2 and 225 K is fairly good, which indicates that the proposed scheme is physically consistent and satisfactory. It is noted that there appears to be a small disagreement, which is of the order of 1–2 % only, between the experimental and theoretical data at very low temperatures. This may be due to various reasons including lattice changes at very low temperatures, variation (i.e., slight increase) of the velocity of sound at low temperatures, and slight structural changes.

## X. REMARKS

As already mentioned, the magnetic susceptibility of $Fe^{2+}$ in deoxyhemoglobin corresponds to spin $S=2$, whereas the observed magnetic hyperfine field ($\sim 11$ T) is considerably less than what can be usually expected from $S=2$. However, the vibronic coupling may produce the desired result in a physically acceptable qualitative manner. An antisymmetric displacement of the appropriate ligands around $Fe^{2+}$ can produce a small admixture between its occupied $3d$ and empty $4p$ orbitals, and the modified orbital function will take the form[38,39]

$$\psi_{3d} = |3d\rangle + \frac{\langle 3d|(\delta V/\delta r)dr|4p\rangle}{E_{3d} - E_{4p}}|4p\rangle \ , \qquad (25)$$

where $(E_{3d} - E_{4p})$ is the energy difference between $3d$ and $4p$ electronic orbital states of the ferrous ions. This scheme, known as the orbital mixing mechanism, is well established in giving rise to dynamic exchange interaction. Though this mixing will be quite small, it can reduce the magnetic hyperfine field in a significant manner by a reduced screening of $3s$ electrons. In effect, the Fermi contact field (at the Fe nucleus) due to polarized $3s$ electrons becomes significantly greater and this will reduce the magnitude of the net contact field.[40] In this picture the magnetic susceptibility will still correspond to the spin $S=2$, (i.e., vibronic coupling does not change the spin). This type of mixing will also reduce by a constant factor the value of the quadrupole splitting due to $3d$ electrons, but that will not be manifested in its temperature dependence. We find that the temperature dependence of $Fe^{2+}$ in deoxymyoglobin and its structurally similar synthetic analogues can be explained in a similar way with minor changes in various parameters.

## ACKNOWLEDGMENT

The author acknowledges the financial support of Council of Scientific and Industrial Research (New Delhi), India.

[1]H. Eicher and A. Trautwein, J. Chem. Phys. **50**, 2540 (1969); **52**, 932 (1970).
[2]A. Trautwein, H. Eicher, and A. Mayer, J. Chem. Phys. **52**, 2473 (1970).
[3]M. F. Perutz, Nature **228**, 726 (1970).
[4]N. Nakano, J. Otsuka, and A. Tasaki, Biochim. Biophys. Acta **236**, 222 (1971); **278**, 355 (1972).
[5]B. H. Huynh, G. C. Papaefthymion, C. S. Yen, J. L. Groves, and C. S. Wu, J. Chem. Phys. **61**, 3750 (1974).
[6]U. Gonser, Y. Maeda, A. Trautwein, F. Parak, and H. Formanek, Z. Naturforsch. Teil B **29**, 241 (1974).
[7]Y. Tanabe and S. Sugano, J. Phys. Soc. Jpn. **9**, 767 (1974).
[8]G. Fermi, J. Mol. Biol. **97**, 237 (1975).
[9]R. Zimmermann, Nucl. Instrum. Methods **128**, 537 (1975).
[10]A. Trautwein, R. Zimmermann, and F. E. Harris, Theor. Chim. Acta **37**, 89 (1975).
[11]A. Alpert and R. Banerjee, Biochim. Biophys. Acta **405**, 144 (1975).
[12]Y. Maeda, T. Harami, A. Trautwein, and U. Gonser, Z. Naturforsch. Teil B **31**, 487 (1976).
[13]H. Eicher, D. Bade, and F. Parak, J. Chem. Phys. **64**, 1446 (1976).
[14]K. Spartalian, G. Lang, and T. Yonetani, Biochim. Biophys. Acta **428**, 281 (1976).
[15]M. Bacci, Chem. Phys. Lett. **48**, 184 (1977); J. Chem. Phys. **68**, 4907 (1978).
[16]W. A. Eaton, L. K. Hanson, P. J. Stephens, J. C. Sutherland, and J. B. R. Dunn, J. Am. Chem. Soc. **100:16**, 4991 (1978).
[17]P. M. Champion and A. J. Sievers, Bull. Am. Phys. Soc. **24**, 3 (1979).
[18]T. A. Kent, K. Spartalian, G. Lang, and T. Yonetani, Biochim. Biophys. Acta **490**, 331 (1977).
[19]T. A. Kent, K. Spartalian, G. Lang, T. Yonetani, C. A. Reed, and J. P. Collman, Biochim. Biophys. Acta **580**, 245 (1979).
[20]T. A. Kent, K. Spartalian, and G. Lang, J. Chem. Phys. **71**, 4899 (1979).
[21]B. H. Huynh and T. A. Kent, in *Advances in Mössbauer Spectroscopy*, edited by B. V. Thosar *et al.* (Elsevier, Amsterdam, 1983) p. 490.
[22]K. K. P. Srivastava, Phys. Rev. B **29**, 4890 (1984); **32**, 3282 (1985).
[23]K. K. P. Srivastava and S. N. Choudhary, Phys. Status Solidi B **134**, 289 (1986).
[24]S. N. Choudhary, T. P. Sinha, and K. K. P. Srivastava, Phys. Status Solidi B **137**, 255 (1986).
[25]T. P. Sinha, S. N. Choudhary, and K. K. P. Srivastava, Phys. Status Solidi B **142**, 221 (1987).
[26]K. K. P. Srivastava and T. P. Sinha, J. Phys. (Paris) **48**, 2119 (1987).
[27]T. P. Sinha, Phys. Status Solidi B **169**, 561 (1992).
[28]R. M. Golding, *Applied Wave Mechanics* (Van Nostrand, London, 1969) p. 177.
[29]B. Bleaney and K. W. H. Stevens, Rep. Prog. Phys. **16**, 108 (1953).
[30]M. T. Hutchings, Solid State Phys. **16**, 227 (1964).
[31]R. Orbach, Proc. R. Soc. London Ser. A **264**, 458 (1961).
[32]M. Zerner, M. Gouterman, and H. Kobayshi, Theor. Chim. Acta **6**, 363 (1966).
[33]F. Varret and G. Jehanno, J. Phys. (Paris) **36**, 415 (1975).
[34]R. Ingalls, Phys. Rev. **133**, A787 (1964).
[35]D. C. Price, Aust. J. Phys. **31**, 397 (1978).
[36]J. M. Ziman, *Electrons and Phonons* (Oxford University Press, Clarendon, England, 1960), p. 181.
[37]C. Y. Huang, Phys. Rev. **139**, A241 (1965).
[38]K. P. Sinha and U. N. Upadhyaya, Phys. Rev. **127**, 432 (1962).
[39]K. P. Sinha and N. Kumar, *Interactions in Magnetically Ordered Solids* (Oxford University Press, Oxford, England, 1980) p. 106.
[40]R. E. Watson and A. J. Freeman, Phys. Rev. **123**, 2027 (1961).